Popular Summary:

"A Geostatistical Data Fusion Technique for Merging Remote Sensing and Ground-based Observations of Aerosol Optical Thickness"

A. Chatterjee, A. M. Michalak, R. A. Kahn, S. R. Paradise, A. J. Braverman, C. E. Miller, 2010.

J. Geophys. Res., 115, D20207, doi:10.1029/2009JD013765, *in press*.

Particles in the atmosphere reflect incoming sunlight, tending to cool the Earth below. Some particles, such as soot, also absorb sunlight, which tens to warm the ambient atmosphere. Aerosol optical depth (AOD) is a measure of the amount of particulate matter in the atmosphere, and is a key input to computer models that simulate and predict Earth's changing climate. The global AOD products from the Multi-angle Imaging SpectroRadiometer (MISR) and the MODerate resolution Imaging Spectroradiometer (MODIS), both of which fly on the NASA Earth Observing System's Terra satellite, provide complementary views of the particles in the atmosphere. Whereas MODIS offers global coverage about four times as frequent as MISR, the multi-angle data makes it possible to separate the surface and atmospheric contributions to the observed top-of-atmosphere radiances, and also to more effectively discriminate particle type. Surface-based AERONET sun photometers retrieve AOD with smaller uncertainties than the satellite instruments, but only at a few fixed locations. So there are clear reasons to combine these data sets in a way that takes advantage of their respective strengths.

This paper represents an effort at combining MISR, MODIS and AERONET AOD products over the continental US, using a common spatial statistical technique called kriging. The technique uses the correlation between the satellite data and the "ground-truth" sun photometer observations to assign uncertainty to the satellite data on a region-by-region basis. The larger fraction of the sun photometer variance that is duplicated by the satellite data, the higher the confidence assigned to the satellite data in that region. In the Western and Central US, MISR AOD correlation with AERONET are significantly higher than those with MODIS, likely due to bright surfaces in these regions, which pose greater challenges for the single-view MODIS retrievals. In the east, MODIS correlations are higher, due to more frequent sampling of the varying AOD. These results demonstrate how the MISR and MODIS aerosol products are complementary. The underlying technique also provides one method for combining these products in such a way that takes advantage of the strengths of each, in the places and times when they are maximal, and in addition, yields an estimate of the associated uncertainties in space and time.

A Geostatistical Data Fusion Technique for Merging Remote Sensing and Ground-based Observations of Aerosol Optical Thickness

A. Chatterjee[1], A. M. Michalak[1,2], R. A. Kahn[3], S. R. Paradise[4], A. J. Braverman[4],C. E. Miller[4]

[1]Department of Civil and Environmental Engineering, University of Michigan, Ann Arbor

[2]Department of Atmospheric, Oceanic and Space Sciences, University of Michigan, Ann Arbor

[3]NASA Goddard Space Flight Centre, Greenbelt, Maryland

[4]Jet Propulsion Laboratory, Pasadena, California

ABSTRACT

The Multi-angle Imaging SpectroRadiometer (MISR) and the Moderate Resolution Imaging 6SHFWURUDGLRPHWHU□□02',6□□DERDUG□WKH□1$6$□(DUWK□2EVHUYDWLRQ□6\VWHP¶V□7HUUD measuring aerosol optical thickness (AOT) since early 2000. These remote-sensing platforms complement the ground-based AErosol RObotic NETwork (AERONET) in better understanding the role of aerosols in climate and atmospheric chemistry. To date, however, there have been only limited attempts to exploit the complementary multiangle (MISR) and multispectral (MODIS) capabilities of these sensors along with the ground-based observations in an integrated analysis. This paper describes a geostatistical data fusion technique that can take advantage of the spatial autocorrelation of the AOT distribution, while making optimal use of all available datasets. Using Level 2.0 AERONET, MISR and MODIS AOT data for the contiguous US, we demonstrate that this approach can successfully incorporate information from multiple sensors, and provide accurate estimates of AOT with rigorous uncertainty bounds. Cross-validation results show that the resulting AOT product is closer to the ground-based AOT observations than either of the individual satellite measurements.

1 INTRODUCTION

Atmospheric aerosols play an important and dynamic role in climate and atmospheric chemistry. The climatic effects of aerosols had already been recognized in the 1970s [*Andreae*, 1995] but the focus of scientific attention shifted only during the late 1980s due to the impact of the growing concentrations of CO_2 and other greenhouse gases. Although the radiative forcing of aerosols is still highly uncertain [*IPCC*, 2007], it is well understood that aerosols contribute significantly to reflected solar radiation (the aerosol direct effect) and modify cloud properties (the aerosol indirect effect), producing a net cooling of the Earth surface, and can also absorb sunlight, thereby warming the ambient atmosphere. Because aerosols have short atmospheric lifetimes of about a week [*Andreae*, 1986], they have a heterogeneous spatial and temporal distribution. Accurately capturing this heterogeneity, and assessing the impact of tropospheric aerosols on regional and global energy budgets, therefore requires diurnally resolved observations from some combination of satellite and suborbital measurements.

Two space-based instruments that aim to fulfill this need are the Multi-angle Imaging SpectroRadiometer (MISR) and Moderate Resolution Imaging Spectroradiometer (MODIS) aboard the NASA Earth Observation System's Terra satellite, which are used to derive observations of the tropospheric aerosol optical thickness (AOT), among other parameters [*Diner et al.*, 1998; *Kaufman et al.*, 1997]. Column AOT is defined as the integral of aerosol extinction from the surface to the top of the atmosphere. Although these two sensors are on the same platform, discrepancies exist between them in retrieved AOT over both land and ocean regions [*Penner et al.*, 2002; *Myhre et al.*, 2005; *Kinne et al.*, 2006]. These discrepancies are due to the differences in assumptions in the retrieval algorithms [*Kahn et al.*, 2007], observed wavelengths and viewing geometries [*IPCC*, 2007], and the spatial resolution of observations [*Xiao et al.*, 2009], among other reasons. Methods for evaluating data from these and other instruments are needed, as are approaches for assessing the information content of these data for providing the best possible representation of the spatial and temporal variability in AOT.

The common way of validating the satellite AOT retrievals has been through the use of the ground-based Aerosol Robotic Network (AERONET; *Holben et al.*, 1998), which provides sparse but relatively reliable AOT observations. Comparisons between AOT retrieved from space-based instruments and AERONET data have been used in a variety of contexts to explore the similarities and differences between the MISR and MODIS products. These comparisons have focused on MISR and AERONET [*Liu et al.*, 2004a; *Kahn et al.*, 2005a, 2005b; *Jiang et al.*, 2007; *Chen et al.*. 2008], or MODIS and AERONET [*Chu et al.,* 2002; *Levy et al.,* 2003, 2005; *Remer et al.,* 2005], and have been specifically targeted at refining the retrieval algorithms of the individual sensors for different aerosol regimes.

Several studies have also looked at the discrepancies between MISR and MODIS [e.g., *Abdou et al.*, 2005; *Liu et al.*, 2007; *Prasad and Singh*, 2007; *Vermote et al.*, 2007; *Xiao et al.*, 2009; *Kahn et al.,* 2009], mostly by comparing them with the AERONET measurements. These studies have concluded that the major differences can be attributed to location (for example, retrievals near aerosol source regions and/or presence of clouds, retrievals over land versus water) and the aerosol retrieval algorithms over those locations. Recently, *Kahn et al.* [2009] compared MISR and MODIS datasets, and found strong correlations of 0.9 and 0.7 between MISR and MODIS over ocean and land, respectively. Discrepancies between the instruments were traced back to sampling differences, known algorithmic issues, or other mechanisms contributing to aerosol retrieval error. Some of these mechanisms that have been highlighted previously are aerosol model differences [*Abdou et al.*, 2005; *Kahn et al.*, 2007], presence of clouds [*Martonchik et al.*, 2004; *Kahn et al.*, 2007; *Xiao et al.* 2009; *Kahn et al., 2009*], dust [*Kalashnikova and Kahn*, 2006; *Martonchik et al.*, 2004], biomass burning [*Kahn et al.*, 2005a; *Chen et al.*, 2008], and other biospheric and anthropogenic factors [*Prasad and Singh*, 2007; *Xiao et al., 2009*]. Statistical comparisons have also been carried out between MISR, MODIS and AERONET by *Liu and Mishchenko* [2008] and *Mischenko et al.* [2009], although some of the statistical techniques used have subsequently been questioned [e.g., *Kahn et al.,* 2009]. Overall, the existing literature has resulted in a complex set of conclusions regarding the ways in which MISR, MODIS, and AERONET record AOT [*Xiao et al*., 2009]. For example, *Liu et al.* [2007] conclude that MODIS generally retrieves higher AOT relative to MISR over land, whereas both MODIS and MISR tend to underestimate AERONET AOT measurements for AOT higher than about 0.5. Similar underestimation is reported by *Jiang et al.* [2007] and *Kahn et al.* [2005a], whereas others conclude that MISR overestimates AERONET AOT observations over water [e.g., *Abdou et al*., 2005; *Kahn et al*., 2005b; *Liu et al.,* 2004a].

Given the limitations inherent to each of the available data streams, combining multiple data types may provide an opportunity to optimally estimate the spatial and temporal distribution of AOT. Some studies have found the correlation between the AOT data from multiple sensors to be sufficiently strong to justify the use of ground-based and space-based observations together [*Liu et al*., 2004a; *Prasad and Singh*, 2007; *Jiang et al*., 2007]. However, most of the data fusion attempts have been limited to merging data from multiple space-based instruments, including Level 1B (i.e. radiance) data [*Loeb et al*., 2006], Level 2 data of geophysical parameters [*Gupta et al*., 2008] and aerosol optical depth [*Nguyen* 2009], and gridded level 3 datasets [*Acker et al*., 2007]. Recently, *Kinne* [2009] presented an approach for integrating a weighted composite of remote sensing AOT observations with AERONET AOT through an empirical averaging procedure.

Given the complementary capabilities of the AERONET, MISR and MODIS sensors (see Section 2), it seems natural to investigate whether it is possible to merge data from these different sensors in a statistically rigorous framework to obtain an improved AOT product. Such a product could be used to address scientific issues related to air quality and the radiative effects of aerosols, and in particular, be used to evaluate model predictions of aerosol distributions.

The objective of this work is to investigate the applicability of Universal Kriging, a simple geostatistical data fusion approach, for merging multiple AOT datasets. The approach yields a statistical best-estimate of the AOT spatial distribution, together with a quantification of the associated uncertainty. The estimated AOT distribution is based only on the available AOT data, and does not incorporate information or assumptions about atmospheric transport or source regions. Given that the availability of multiple satellite datasets has already resulted in a research shift from modeling-only to observational-based assessments of aerosol forcing [*Yu et al.*, 2006], geostatistical data fusion can potentially provide useful optimal fused datasets, taking advantage of the strengths, and minimizing the limitations, of each individual sensor in a new way.

The remainder of this paper is organized as follows. Section 2 provides a description of the MISR, MODIS and AERONET data used in the presented analysis. Section 3 gives an overview of the applied method and examined test cases. Results are presented and discussed in Section 4.

2 DATA

The description of the datasets presented here covers only the specific data products used in this study. The reader is referred to *Martonchik et al.* [2009] and *Remer et al.* [2009] for descriptions of the retrieval algorithms and *Yu et al.* [2006] for an overview of how tropospheric aerosols are measured. All analyses are performed using data from 2001.

2.1 AERONET

AERONET is a globally distributed network of over 200 automated ground-based instruments covering all major tropospheric aerosol regimes [*Holben et al*., 1998; 2001]. The instruments used are CIMEL sun/sky radiometers that make direct sun measurements with a 1.28Ûfull field-of-view every 15 minutes in eight spectral bands [*Holben et al*., 1998]. Level 2 (validated) AOT data are used here for 32 sites within the continental United States. The AERONET data archive (http://aeronet.gsfc.nasa.gov), includes AOT at diffHUHQW□ZDYHOHQJWKV□□UHODWLYH□HUURUV□RI□$27□□$QJVWURP□H[SRQHQWV□□

resolution of the dataset is 17.6 km. Theoretical sensitivity studies for MISR [*Kahn et al.,* 2001] have estimated the standard deviations of the measurement error associated with the optical depth to be 0.05

□RU□□□□

The AOT data from the three sensors cannot be compared directly, in part because they are reported at different spatial resolutions. Therefore, following the methodology of *Liu et al.* [2004a], the mean of MISR and MODIS observations within a 0.5° by 0.5° bounding box around each AERONET site is used as a basis for comparison to AERONET data, which are themselves averaged over ±30 min from the Terra overpass. Correlation coefficients are used to characterize the agreement between daily data-pairs from the 32 AERONET sites and the corresponding MISR or MODIS observations at those sites.

3.2 Investigation of the Spatial and Temporal Variability in MISR and MODIS AOT

AOT varies spatially and temporally. This variability can be quantified using variogram analysis, a geostatistical spatial analysis tool. Although the AERONET network is too sparse to independently characterize the spatial variability at the continental scale, it can be used for regional analyses in areas when the network is relatively dense. On the other hand, the dense MISR and MODIS data coverage provides good information about AOT spatial variability as captured by these instruments. Analysis of the MISR and MODIS AOT spatial variability provides insights into differences in the way that these instruments capture the AOT distribution. Differences may be due to the differences in the observational spatial resolution and sampling, instrument signal-to-noise ratios, or retrieval algorithms.

For assessing the AOT temporal variability, the AERONET network is the better candidate, due to its frequent temporal sampling during daylight hours, unlike the snapshots from MISR and MODIS. However, when the spatial and temporal variability is examined simultaneously, the MISR and MODIS AOT retrievals can also provide useful information about space-time variability. For simplicity, the spatial and temporal analysis is presented here using the MISR and MODIS data, but the conclusions about the temporal variability are consistent with those obtained using the AERONET observations (results not shown). The temporal component of the analysis is useful for identifying the timescales over which the AOT data can be integrated into relatively contiguous maps without introducing errors due to correlations in the temporal variability of the AOT.

The spatiotemporal correlation analysis is performed using variogram analysis (e.g., *Chiles and Delfiner, 1999*). For all pairs of AOT data from a given instrument (e.g. MISR), the raw variogram is evaluated as:

$$\frac{1}{\ } \qquad {}^{2} \tag{2}$$

where z are the AOT observations at locations x_i and x_j and times t_i and t_j, h_x is the spatial separation distance between the two observation locations, and h_t is the temporal lag in days between the observations. h_x is calculated as the great circle distance between the locations x_i and x_j

$$h_x(x_i, x_j) = r\cos^{-1}\ \sin\phi_i \sin\phi_j + \cos\phi_i \cos\phi_j \cos(\theta_i - \theta_j) \tag{3}$$

where (ϕ_i, θ_i) are the longitude and latitude of location x_i and r is the Earth's mean radius. In the analysis presented here, a raw variogram is created for each repeat cycle of MODIS and MISR (i.e. each available 16 day period in 2001).

Once the raw variograms are obtained, the variability can be visualized by binning the variances γ into preset ranges of separation distances (h_x) and time lags (h_t). The binned version of the raw variogram is referred to as the experimental variogram. If the temporal correlation of the observations across multiple days is negligible, the experimental variogram can be presented as a function of spatial lag only, and a theoretical model can be selected to represent the observed spatial-only variability. In the analyses presented here, an exponential model was found to represent the spatial correlation of the AOT data well:

$$0 \qquad 0$$

$$^{2} \quad ^{2} \qquad — \qquad (4)$$

where σ^2 $(=\sigma_n^2+\sigma_b^2)$ represents the variance of observed AOT at large separation distances (i.e., for uncorrelated observations) and l is the range parameter. The correlation length beyond which correlation between points becomes negligible is defined as approximately $3l$ [e.g., *Chiles and Delfiner*, 1999]. σ_n^2 is the nugget, representing both the measurement error and the small-scale variability at distances smaller than those resolved by available observations, whereas σ_b^2 represents the variance of the portion of the AOT variability that is spatially correlated. These parameters are optimized using a least squares fit to the spatial raw variogram. Conceptually, a higher variance is indicative of greater overall variability, and a shorter correlation length indicates greater spatial variability at smaller scales.

3.3 Geostatistical Data Fusion Approach

Universal kriging (e.g., *Chiles and Delfiner, 1999*), a geostatistical data fusion approach, makes it possible to fuse auxiliary variables with full spatial coverage (e.g. MISR and MODIS AOT) to improve the interpolation of a primary dataset with observations at a finite number of locations (e.g. AERONET AOT). The auxiliary variables fill a role analogous to regressors in multiple linear regression, but within a framework that accounts for the spatial correlation of the estimated field, and can reproduce observed AERONET AOT measurements exactly at sampling locations.

The objective is to estimate the AOT distribution (**s**) at m locations and times (typically defined on a regular grid), given the AERONET AOT measurements at n locations and times, where **s** ($m \times 1$) is modeled as the sum of a deterministic but unknown component $\mathbf{X_s}$

AOT observations. At the estimation locations, this component represents the predicted residuals between the true AOT and the weighted MISR and MODIS AOT at those locations/times. The covariance of these residuals is described using a matrix **Q**, where the covariance function is defined based on the variogram analysis (Equation 4), such that the covariance between two points x_i and x_j is defined as:

$$
{}^{2} \quad {}^{2} \quad {}^{2} \quad {}^{2} \quad \_\_ \tag{7}
$$

In this case, the variogram analysis is carried out on the detrended AERONET AOT data ($\mathbf{z} \pm \mathbf{X_s}$

where $\mathbf{Q}_{\mathbf{zz}}$ is the $n \times n$ spatial covariance matrix defined between AERONET observation locations based on Equation 7, $\mathbf{X}_{\mathbf{z}}$ $(n \times p)$ is the trend term defined at the measurement locations based on Equation 6, $\mathbf{Q}_{\mathbf{zs}}$ $(n \times m)$ represents the covariance evaluated between the measurement and the estimation locations again based on Equation 7, and $\mathbf{X}_{\mathbf{s}}$ $(m \times p)$ is the model of the trend defined at the estimation locations again based on Equation 6.When multiple time periods are used in the analysis, as is true for the test cases described in Section 3.4, the correlation between time periods is assumed to be zero. The system of equations is solved for $\mathbf{M}$, a $p \times m$ matrix of Lagrange multipliers, and where the diagonal elements of $_{0}$ represent the uncertainty of the individual drift parameters, and the off-diagonal terms represent the estimated covariance of the errors associated with these estimates. Recall that the drift coefficients are the weights assigned to the MISR and MODIS AOT datasets. These weights remain constant over the domain of analysis. As a consequence, the relationship between the true (as represented by AERONET) AOT, and MISR and MODIS AOT, is implicitly assumed to remain constant within an examined region. This is one of the reasons for which the test cases examined in Section 3.4 are conducted regionally, because the relationship between MISR, MODIS, and AERONET cannot necessarily be assumed to remain constant throughout the continental United States.

Ordinary Kriging, a simple geostatistical interpolation technique, is used for comparison to the Universal Kriging estimates in the presented analyses. Ordinary kriging is one of the most commonly used techniques in geostatistical gap filling, but it lacks the advantage of using information from multiple sensors. In the ordinary kriging approach, $\mathbf{X}_\mathbf{s} = [1...1]^T$, and the covariance is derived using a variogram of the AERONET observations without detrending. The other equations remain unchanged. Past applications of ordinary kriging in aerosol science have been limited to estimation of aerosol species over different regions [*Zapletal*, 2001; *Delalieux et al.*, 2006], and have not been aimed at comparison with other estimation techniques. In this work, because the true AOT distribution is unknown, the ordinary kriging estimates are used as a baseline for evaluating the estimates from universal kriging. By comparing the two kriging estimates, we identify the effect of using additional satellite observations on both the AOT estimates and the uncertainty associated with those estimates.

3.4 Test Cases

The correlation analysis (Section 3.1) is carried out for three regions over the contiguous United States for selected periods in 2001. Recognizing that aerosol distributions can be both site and season specific, the

United States are divided into three regions (Western, Central, and Eastern), as illustrated in Figure 1. In the Western region, we expect dust to be dominant, along with biomass burning during the summer and autumn months. Biogenic aerosols often dominate the southeast, especially in summer, where biomass burning may also be important in some seasons. Four seasons are considered: Winter (DJF), Spring (MAM), Summer (JJA) and Fall (SON). Following previous studies (*Kahn et al.* [2005a]; *Liu et al.* [2004a]; *Abdou et al.* [2005]), the correlation analysis was carried out at a daily scale.

The spatio-temporal analysis is carried out using the MISR and MODIS datasets. The analysis is performed at the native resolution of MISR (i.e., 17.6 km) and MODIS (i.e., 10 km) AOT for each 16-day repeat cycle of the Terra satellite in 2001. By doing this analysis for each 16-day repeat cycle, the seasonal changes in spatio-temporal variability of AOT can be assessed, as well as how these changes relates to the periodic changes in the underlying AOT processes over the continental US.

Finally, the geostatistical data fusion analysis is presented using two test cases, the first being over the Eastern US during autumn, and the second over the Western US during summer (Figure 2). Table 1 outlines the details of these two test cases. For these test cases, the study region is broken up into $0.2° \times 0.2°$ grid cells at which the AOT estimates are obtained. The MISR and MODIS observations used for this analysis are averages of all the MISR and MODIS AOT observations falling within a given $0.2° \times 0.2°$ grid cell. This particular estimation resolution is chosen to show the flexibility of the universal kriging approach in estimating AOT at very fine resolutions, but in general could be performed at coarser estimation scales as well.

As will be shown in Section 4.2, there is little significant temporal correlation in the day-to-day variability in the MISR and MODIS AOT within a 7-day period. As a result, the geostatistical data fusion is performed in one-week increments, using weekly-averaged AOT data from AERONET, MISR and

MODIS. These averaged AOT data are used to obtain estimates of the average spatial distribution of AOT over those 7-day periods. For each 7-day period, AERONET sites that have AOT data for at least three of the seven days, and which have overlapping MISR and MODIS data, are used in the analysis. As a result, for the Eastern Test Case during autumn, two to ten sites are used during the various weeks, whereas for the Western Test Case during summer, two to eight sites are used in each week. Figure 2 shows the locations of all the sites used in the test cases. It should be noted here that there may be cases in which significant temporal correlation may exist (e.g. near sources), such as where shorter time-scale variations are predominant, or where strong gradients occur in transported aerosol from far sources. In such cases the data fusion approach should be applied with caution.

The AOT estimates obtained from universal kriging (henceforth denoted as AOT_{UK}) are compared with AOT estimates obtained from ordinary kriging (henceforth denoted as AOT_{OK}). Cross-validation is used to compare the two estimates. In this approach, individual AERONET 7-day observations at a given site are sequentially eliminated from the analysis, and estimates at these locations and times are obtained using the remaining AERONET observations, and, for AOT_{UK}, using available MISR and MODIS data as well. Because AERONET measurements have traditionally been used for validating satellite observations of MISR and MODIS [*Kahn et al.*, 2005a; *Remer et al.*, 2005; *Yu et al.*, 2006], the withheld AERONET observations are used to evaluate the relative precision and accuracy of the AOT_{OK} and AOT_{UK} estimates.

The evaluation of AOT_{OK} and AOT_{UK} estimates is carried out using three metrics. First, the root mean square error (RMSE) is calculated between the estimated AOT and the AERONET observations. Second, the magnitude of the predicted kriging uncertainties is evaluated by calculating the root mean square prediction error (RMSPE) of the kriging uncertainties (Equation 10). Third, the accuracy of these predicted uncertainties is evaluated by verifying the percent of true AERONET AOT observations that fall within two standard deviations of the estimated AOT, where the standard deviations are those predicted by the kriging analyses (Equation 10). This third metric is less sensitive to extreme outliers, and, in an ideal scenario, 95% of the true AOT should fall within this interval. Values significantly below 95% would indicate an underestimation of the true uncertainties, while values substantially above 95% indicate overly conservative estimates. All three metrics are calculated across the entire season for both test cases.

Overall, the two examined test cases are designed to (i) demonstrate the versatility of the universal kriging technique in estimating AOT over different regions and across seasons, (ii) evaluate the improvement of universal kriging estimates over ordinary kriging estimates (or simply the AOT fields observed by MISR or MODIS individually) as a function of the strength of the relationship between MISR, MODIS, and AERONET AOT.

4 RESULTS AND DISCUSSION

4.1 Comparison of MISR, MODIS and AERONET datasets

The results of the correlation analysis are presented in Table 2, and reveal that MISR data have a stronger correlation to AERONET data (ρ=0.47 to 0.92) than do MODIS data (ρ=0.09 to 0.61) across seasons in the Western and Central regions. Given that the correlation coefficient is an indication of the degree of linear covariability between the datasets, this implies that MISR is better able to explain the variability in the AERONET AOT than MODIS over these regions. Note that for MODIS, the "standard" product was used in this paper, and it is plausible that using the more recent "Deep Blue" product, which was not available at the time of analysis, would have shown better agreement with the AERONET AOT, at least over bright surfaces. On the other hand, the particle properties used in the MODIS standard AOT retrieval over land are assumed based on AERONET values [*Levy et al.,* 2007], whereas for MISR, particle properties are retrieved along with AOT as part of a self-consistent process [*Martonchik et al.,* 2009].

The weak correlation in the Western region for both instruments is primarily due to low AOT values in this region, which are near the lower limit of retrieval sensitivity for MISR and MODIS. *Liu et al.* [2004a; 2004b] points out that low values of AOT, as well as coarse-particle dominated scenarios, may produce poor correlations with AERONET AOT. This does not necessarily indicate poor MISR or MODIS performance; rather, at very low AOT values, the correlation coefficients are not informative because the uncertainty associated with the satellite retrievals is large compared to the magnitude of the AOT itself. The high surface albedo in the Western sector and the frequent atmospheric loading with non-spherical mineral dust are additional obstacles to obtaining good satellite retrievals of AOT over this region.

In the Eastern region, the MISR (ρ=0.52 to 0.86) and MODIS (ρ=0.70 to 0.87) data show comparable correlations to AERONET across seasons, and are able to capture the AERONET AOT variability better than across the other two examined regions. The year-round correlation coefficients (ρ = 0.78 for MISR and ρ=0.84 for MODIS) are similar to values that have been reported previously for continental sites in this region [*Chu et al*., 2002; *Liu et al*., 2004a; *Kahn et al*., 2005a].

Overall, results from this analysis are consistent with previous findings that indicate that differences between MISR and MODIS AOT relative to AERONET AOT are caused by site-specific effects and aerosol-size-distribution effects.

This initial analysis indicates that the information provided by MISR and MODIS with regard to the AOT distribution as measured by the AERONET network varies regionally and seasonally throughout the continental United States. Based on these results, it is expected that universal kriging analysis should outperform ordinary kriging in the Eastern region, where the correlations between the AERONET data and the MISR and MODIS data are strong. In other regions, the additional information provided by MODIS and MISR is less significant, and the universal kriging and ordinary kriging analyses are expected to be more similarly to one another.

4.2 Spatio-Temporal Variability Analysis

The spatio-temporal variability analysis is performed for MISR and MODIS AOT for each 16-day repeat cycle in 2001 for the Terra satellite. For each repeat cycle, a spatio-temporal experimental variogram is obtained. Example variograms are presented for MISR and MODIS in Figures 3a and 3b, for April 11 to 26, 2001. These variograms represent the expected variance of pairs of MISR (Figure 3a) or MODIS (Figure 3b) observations, separated by a given distance in space and time lag.

Figures 3a and 3b do not exhibit any noticeable temporal correlation in the day-to-day variability of the AOT distribution for time lags up to 7 days. The temporal lag (shown on the vertical axis) in Figures 3a and 3b represents the number of days between the times when two observations are recorded. A temporal lag of one day could therefore represent, for example, the expected variance between observations taken on days 14 and 15, or on days 1 and 2 or the repeat cycle. The lack of temporal correlation indicates that the coherent temporal variability in the AOT takes place either at sub-diurnal scales that cannot be captured by the examined remote sensing data products, and/or at longer time scales, potentially representative of seasonal variability.

Hence, the results of this analysis indicate that temporal correlation is not significant at for time lags up to 7 days, and therefore that MISR and MODIS data taken over a week can be integrated into a single map. In other words, multiple days of data can be used concurrently to inform the data fusion analysis.

Note that the lack of temporal correlation does not necessarily imply a lack of temporal variability, but simply that the observed AOT is not correlated from day to day.

On the other hand, Figures 3a and 3b reveal that the MISR and MODIS AOT data do exhibit strong spatial correlation, as evidenced by the fact that the variance increases as the spatial separation distance increases. This is more clearly visible in Figures 3c and d, where all data from the April 11 to 26 repeat cycle are examined in a single spatial variogram. These figures display both the experimental and the fitted theoretical spatial variograms for MISR and MODIS. These two figures indicate that the correlation length of AOT data (i.e., the lag distance at which the semivariance reaches an asymptote) appears to be approximately 900km for both instruments for the examined time period, indicating that observations separated by longer distances are essentially independent.

Figures 3e and 3f present the parameters of the fitted theoretical spatial variograms for each of the 25 Terra repeat cycles in 2001. This analysis shows that the spatial correlation of the MISR and MODIS AOT data are quite consistent with one another (blue lines in Figures 3e and f). The correlation lengths vary significantly throughout the year, ranging from 500km to 1500km, with higher values prevalent during the summer months. On the other hand, the total amount of variability (i.e. variance) of the MODIS AOT is always significantly higher than that of MISR. During the winter months, both MISR and MODIS show shorter correlation lengths and increased variance, representative of a more heterogeneous distribution of aerosols. In general, the long-range transport of dust in late spring and summer, and smoke from summer through early autumn, are likely to contribute to the longer correlation lengths during the summer months, whereas local aerosol sources explain the smaller-scale variability observed during other seasons.

Seasonal changes in the spatial variability of AOT will impact the uncertainty estimates obtained from universal kriging. During the summer months, due to the longer correlation lengths and smaller variance, the AOT estimates will have lower uncertainty, while, conversely, during the winter months, we can expect higher estimation uncertainties.

One interesting conclusion from Figure 3 is that the MODIS AOT variance is higher than that for MISR, across all seasons. This is due in part to the fact that the more frequent and finer scale MODIS sampling captures more small-scale AOT variability than MISR. The second reason for this higher variance is that, due to its exclusively near-nadir viewing geometry, MODIS has a greater sensitivity to variability in surface brightness on small spatial scales, which in turn introduces some additional variability into the MODIS AOT retrievals. Neither of these features hinders the application of the universal kriging approach presented in this work. However, it has implications for researchers pursuing assimilation of MISR and MODIS radiance data, or looking to improve the retrieval algorithms of these two sensors.

4.3 Data Fusion Results

Figures 4 and 5 show the estimated AOT field for one week of each of the case studies described in Table 1. The Eastern test case demonstrates that the universal kriging AOT estimates are better than the ordinary kriging estimates when MISR and MODIS are significantly correlated with the AERONET AOT observations. The associated uncertainties for the AOT_{UK} estimates are significantly lower. Cross-validation at the AERONET locations confirms that the AOT_{UK} estimates are more realistic than the AOT_{OK} estimates, as shown for one of the 7-day periods in Figure 6 (see Figures S1 and S2 in the Supplementary material for the entire season). Overall, for this test case, the RMSE for AOT_{UK} is 0.053, which is lower than that of AOT_{OK} (0.067) and each of the individual satellite datasets (0.054 for MISR and 0.056 for MODIS). The true AOT falls within the 2 standard deviations of both the kriging estimates for 93% of AERONET observations, but the RMSPE of AOT_{UK} (RMSPE = 0.035) is significantly lower than that of AOT_{OK} (RMSPE = 0.069). These results confirm that, when strong correlation exists between multiple datasets, the universal kriging approach can be used to obtain better predictions with smaller uncertainties relative to estimates based on measurements from a single sensor. This is evident not only from the reduction in uncertainty, but also from the lower RMSE and RMSPE values of AOT_{UK} relative to $AOT_{OK.}$

The Western test case demonstrates that the universal kriging estimates are comparable to the ordinary kriging estimates in regions where the correlation with MISR and MODIS is low. The predicted uncertainty (Figure 5b and d) is similar for the two methods. This is consistent with our findings from the correlation analysis,, because MISR and MODIS are not strongly correlated with the AERONET AOT in this region (Table 2), and are therefore unable to capture the AERONET AOT variability. Cross-validation results shown in Figure 7 confirm that the two approaches provide similar estimates with high uncertainty (see Figure S3 and S4 in the Supplementary material for the entire season). The AERONET, MISR and MODIS AOT values are also plotted in Figure 7, and demonstrate that, for the examined case, both ordinary and universal kriging seem to do better than just using individual MISR and MODIS datasets. This is further validated by the metrics calculated for the entire season. The RMSE for both AOT_{UK} and AOT_{OK} is 0.047 and 0.048, respectively, which is lower than the RMSE of 0.082 for MISR and 0.26 for MODIS. The true AERONET AOT fall within 2 standard deviations of AOT_{UK} and AOT_{OK} estimates for 98% of available observations. Finally, the RMSPEs are similar for the ordinary (RMSPE = 0.066) and universal (RMSPE = 0.061) kriging approaches, reaffirming their similarity to one another for this test case.

In addition to predicting AOT, the universal kriging approach can be used to quantify which of the satellite observations has more influence on the estimation procedure, by looking at the drift coefficient ($\ddot{O}$) values and their uncertainties ($\sigma_{\ddot{O}}$), as shown in Table 3. A coefficient of variation ($\sigma_{\ddot{O}}/\ddot{O}$) below 0.5 implies a statistically significant contribution to the trend at the 2 $\sigma_{\ddot{O}}$ level. For the Eastern Test Case, the MODIS AOT observations have a more significant drift coefficient ($\sigma_{\ddot{O}}/\ddot{O}= 0.18$) than the MISR data, and these latter data are therefore used primarily to adjust the spatial pattern in MODIS AOT to more closely resemble the AERONET AOT observations. Conversely, for the Western Test Case, the MISR AOT observations seem to be a significant predictor of AERONET AOT measurements ($\sigma_{\ddot{O}}/\ddot{O} = 0.43$). In addition, the drift coefficient values for the constant term ($\ddot{O}_0$) are not significantly different from zero for either examined case, indicating an absence of any systematic offset between the AOT predicted by the weighted combination of MISR and MODIS, and the AOT observed by AERONET.

Finally, although this analysis used both MISR and MODIS in the data fusion process, one could easily use either MISR or MODIS individually, or some other combined AOT product(s). The approach presented combines the best available information from all available sensors to identify the optimal weighted combination to represent the AOT distribution.

5 CONCLUSIONS

A geostatistical data fusion technique is implemented for combining remote-sensing and ground-based observations of AOT. Results show that adopting the universal kriging approach based on the combination of MISR, MODIS and AERONET enables better estimation of AOT with reduced uncertainties, relative to estimates based on observations from a single instrument.

All three examined datasets were found to display strong spatial correlation in their measured AOT distributions. Although the total degree of AOT variability differed between MISR and MODIS, the spatial scales of this variability were similar for these instruments. The day-to-day temporal correlation in MISR or MODIS AOT observations was found to be minimal, due at least in part to limited temporal sampling, making it possible to integrate such observations over multiple days to better infer the spatial distribution of AOT.

As an increasing number of remote sensing observations become available, data fusion approaches such as the one presented here may hold the key to furthering our understanding of atmospheric aerosols. Although differences between instruments are always present, the approach implemented here takes advantage of their complementary features by combining the datasets in a manner that is statistically robust. The approach relies on the availability of auxiliary variables (MISR and MODIS AOT, in the presented analysis) at all locations where the AOT is to be estimated, and assumed that the relationship between these auxiliary variables and the primary observations (AERONET AOT, in the presented analysis) remains constant throughout the examined region.

Finally, this study reinforces the complementary value of remote-sensing and ground-based observations of AOT. Long-term monitoring of aerosol distributions is possible via remote sensing measurements, and these can be used to capture the spatio-temporal distribution of aerosols. Expected refinements in retrieval algorithms and sensor capabilities will improve the accuracy of the retrieved AOT further. By fusing these measurements with ground-based observations using techniques such as the one presented here, it will be possible to obtain reliable long-term estimates of AOT at national and even global scales.

ACKNOWLEDGEMENTS

:H□WKDQN□RXU□FROOHDJXHV□RQ□WKH□-HW AMRS system team for providing us with the MISR and MODIS datasets. We also specially thank three anonymous reviewers and Angela Benedetti for providing us with excellent suggestions and feedback. The authors would also like to thank the AERONET PIs for collecting the aerosol data over the United States. The University of Michigan component of this research was funded through the 'LUHFWRU¶V□5HVHDUFK□DQG□'HYHORSPHQW□)XQG□XQGHU□D□FRQWUDFW□ZLWK□WKH□1DWLRQDO□$H Administration. Additional support was provided through NASA grant NNX08AJ92G. The work of R. Kahn is VXSSRUWHG□LQ□SDUW□E\□1$6$¶V□&OLPDWH□DQG□5DGLDWLRQ□5HVHDUFK□DQG□$QDO\VLV□3URJUDP□ Atmospheric Composition Program, and the EOS-MISR project.

REFERENCES

1. Abdou, W. A., D. J. Diner, J. V. Martonchik, C. J. Bruegge, R. A. Kahn, B. J. Gaitley, K. A. Crean, L. A. Remer, and B. Holben (2005), Comparison of coincident Multiangle Imaging Spectroradiometer and Moderate Resolution Imaging Spectro-radiometer aerosol optical depths over land and ocean scenes containing Aerosol Robotic Network sites, J. Geophys. Res. 110, D10S07, doi:10.1029/2004JD004693.
2. Acker, J. and G. Leptoukh (2007), Online analysis enhances use of NASA Earth science data, Eos Trans. AGU, 88(2), 14±17, 2007.
3. Anderson, T. L. et al. (2005), An A-Train strategy for quantifying direct climate forcing by DQWKURSRJHQLF□DHURVROV Bull. Amer. Meteorol. Soc. 86(12), 1795±1809.
4. Andreae, M. O. (1995), Future Climates of the World, World Survey of Climatology vn. 16, A Henderson-Sellers Ed., 341-392.
5. Andreae, M. O. et al. (1986), External mixture of sea salt, silicates, and excess sulfate in marine aerosols, Science 232, 1620±1623.
6. Chen, W-T, R. Kahn, D. Nelson, K. Yau, and J. Seinfeld (2008), Sensitivity of multi-angle imaging to optical and microphysical properties of biomass burning aerosols, J. Geophys. Res. 113, D10203, doi:10.1029/2007JD009414.
7. Chiles, J.-P., and P. Delfiner (1999), Geostatistics: modeling spatial uncertainty, Wiley-Interscience.
8. Chu, D. A., Y. J. Kaufman, C. Ichoku, L. A. Remer, D. Tanré, and B. N. Holben (2002), Validation of MODIS aerosol optical depth retreival over land, Geophsical Research Letters 29(12), doi:10.1029/2001/GL013205.
9. Delalieux, F., R. van Grieken, J. H. Potgieter (2006), Distribution of atmospheric marine salt depositions over Continental Western Europe, Marine Pollution Bull. 52(6), doi:10.1016/j.marpolbul.2005.08.018, 606-611.
10. Diner, D. J., J. C. Beckert, T. H. Reilly, C. J. Bruegge, J. E. Conel, R. A. Kahn (1998), Multi-angle imaging spectroradiometer (MISR) instrument description and experiment overview, IEEE Transactions on Geosciences and Remote Sensing 36, doi: 10.1109/36.700992, □□□□í□□□□□
11. (FN□□7□□)□□□%□□+ROEHQ□□-□□5HLG□□2□□'XERYLN□□$□□6PLUQRY□□1□□7□□2¶1HLOO (1999), Wavelength dependence of the optical depth of biomass burning, urban, and desert aerosols, J. Geophys. Res. 104(D24), 31,333±31,349.
12. Gupta, P., F. Patadia and S. A. Christopher (2008), Multisensor Data Product Fusion for Aerosol Research, IEEE Trans. on Geoscience and Remote Sensing 46(5), doi: 10.1109/TGRS.2008.916087,1407-1415.
13. Holben, B. N., et al. (2001), An emerging ground-based aerosol climatology: aerosol optical depth from AERONET, J. Geophys. Res. 106, 12067-12098.
14. Holben, B. N., T.F. Eck, I. Slutsker, D. Tanre´, J. P. Buis, A. Setzer, E. Vermote, J. A. Reagan, Y. J. Kaufman, T. Nakajima, F. Lavenu, I. Jankowiak, A. Smirnov (1998), AERONET ± A federated instrument network and data archive for aerosol characterization, Remote Sensing of Environment 66(1), 1-16.
15. Intergovernmental Panel on Climate Change Fourth Assessment Report, Working Group I Report 'The Physical Science Basis', edited by S. Solomon, D. Qin, M. Manning et al. (2007), Cambridge University Press, Cambridge.
16. Jiang, X., Y. Liu, B. Yu, and M. Jiang (2007), Comparison of MISR aerosol optical thickness with AERONET measurements in Beijing metropolitan area, Remote Sensing of Environment 107(1-2), doi:10.1016/j.rse.2006.06.022, 45±53.

17. Kahn, R. A., D. L. Nelson, M. J. Garay, R. C. Levy, M. A. Bull, D. J. Diner, J. V. Martonchik, S. R. Paradise, E. G. Hansen, and L. A. Remer (2009), MISR aerosol product attributes and statistical comparisons with MODIS, IEEE Trans. on Geosciences and Remote Sensing, 47(12), doi: 10.1109/TGRS.2009.2023115, 4095-4114.
18. Kahn, R. A., M. J. Garay, D. L. Nelson, K. K. Yau, M. A. Bull, B. J. Gaitley, J. V. Martonchik, and R. C. Levy (2007), Satellite-derived aerosol optical depth over dark water from MISR and MODIS: Comparisons with AERONET and implications for climatological studies, J. Geophys. Res., 112, D18205, doi:10.1029/2006JD008175.
19. Kahn, R.A., B. Gaitley, J. Martonchik, D. Diner, K. Crean, and B. Holben (2005a), MISR global aerosol optical depth validation based on two years of coincident AERONET observations. J. Geophys. Res. 110, doi:10:1029/2004JD004706.
20. Kahn, R.A., W.-H. Li, J. V. Martonchik, C. J. Bruegge, D. J. Diner, B. J. Gaitley, W. Abdou, O. Dubovik, B. Holben, A. Smirnov, Z. Jin, and D. Clark (2005b), MISR calibration, and implications for low-light level aerosol retrieval over dark water, Journal of the Atmospheric Sciences 62(4), 1032±1052.
21. Kahn, R.A., P. Banerjee, and D. McDonald (2001), The sensitivity of multiangle imaging to natural mixtures of aerosols over ocean, J. Geophys.Res., 106, 18,219± 18,238.
22. Kalashnikova O. V., and R. Kahn (2006), Ability of multiangle remote sensing observations to identify and distinguish mineral dust types: Part 2. Sensitivity over dark water, J. Geophys. Res., 111, D11207, doi:10.1029/2005JD006756.
23. Kaufman, Y. J., D. Tanre′, and O. Boucher (2002), A satellite view of aerosols in the climate system, Nature 419, doi:10.1038/nature01091.
24. Kaufman, Y. J., D. Tanre′, L. A. Remer, E. Vermote, A. Chu, and B. N. Holben (1997), Operational remote sensing of tropospheric aerosol over land from EOS Moderate Resolution Imaging Spectroradiometer, J. Geophys. Res. 102, 17,051±17,067.
25. Kinne, S (2009), Remote sensing data combinations: superior global maps for aerosol optical depth, in Satellite Aerosol Remote Sensing over Land, edited by A. A. Kokhanovsky and G. de Leeuw, Springer, Berlin.
26. Kinne, S., et al. (2006), An AeroCom initial assessment ± optical properties in aerosol component modules of global models, Atmos. Chem. Phys. 6, 1815-1834.
27. Levy, R. C., L.A. Remer, S. Mattoo, E. F. Vermote, Y. J. Kaufman (2007) Second-generation operational algorithm: retrieval of aerosol properties over land from inversion of moderate resolution imaging spectroradiometer spectral reflectance, J. Geophys. Res. 112 (D13), D13211, doi:10.1029/2006JD007811.
28. Levy, R. C., L. A. Remer, J. V. Martins, Y. J. Kaufman, A. Plana-Fattori, J. Redemann, and B. Wenney (2005), Evaluation of the MODIS aerosol retrievals over ocean and land during CLAMS, Journal of. Atmospheric Sciences 62, 974±992.
29. Levy, R. C., L. A. Remer, D. Tanre, Y. J. Kaufman, C. Ichoku, B. N. Holben, J. M. Livingston, P. B. Russell, and H. Maring (2003), Evaluation of the Moderate-Resolution Imaging Spectroradiometer (MODIS) retrievals of dust aerosol over the ocean using PRIDE, J. Geophys. Res. 108(D19), 8594, doi:10.1029/2002JD002460.
30. /LX□□/□□DQG□0□□,□□0LVKFKHQNR□□□□□□□□³7RZDUG□XQLILHG□VDWHOOLWH□FOLPDW sites. 'LUHFW□FRPSDULVRQV□RI□DGYDQFHG□OHYHO□□□DHURVRO□SURGXFWV J. Quant. Spectrosc. Radiat. Transf., □´□ 109(14), 2376±2385, doi:10.1016/j.jqsrt.2008.05.003
31. Liu, Y., M. Franklin, R. Kahn, and P. Koutrakis (2007), Using aerosol optical thickness to predict ground-level PM2.5 concentrations in the St. Louis area: A comparison between MISR and MODIS, Remote Sensing of Environment 107, doi:10.1016/j.rse.2006.05.022,33±44.

32. Liu, Y., J. A. Sarnat, B. A. Coull, P. Koutrakis, and D. J. Jacob (2004a), Validation of Multiangle Imaging Spectro-radiometer (MISR) aerosol optical thickness measurements using Aerosol Robotic Network (AERONET) observations over the contiguous United States, J. Geophys. Res. 109, D06205, doi:10.1029/2003JD003981.
33. Liu, Y., R. J. Park, D. J. Jacob, Q. Li, V. Kilaru, and J. A. Sarnat (2004b), Mapping annual mean ground-level PM2.5 concentrations using Multiangle Imaging Spectroradiometer aerosol optical thickness over the contiguous United States, J. Geophys. Res.109, D22206, doi:10.1029/2004JD005025.
34. Loeb, N.G., W. Sun, W. F. Miller, K. Loukachine, and R. Davies (2006), Fusion of CERES, MISR, and MODIS measurements for top-of-atmosphere radiative flux validation, J. Geophys. Res.111, D18209,doi: 10.1029/2006JD007146.
35. Martonchik, J.V., R.A. Kahn, and D.J. Diner (2009), Retrieval of Aerosol Properties over Land Using MISR Observations, in Satellite Aerosol Remote Sensing Over Land, edited by A. A. Kokhanovsky and G. de Leeuw, Springer, Berlin.
36. Martonchik, J. V., D. J. Diner, R. Kahn, B. Gaitley, and B. N. Holben (2004), Comparison of MISR and AERONET aerosol optical depths over desert sites, Geophysical Research Letters 31, L16102.
37. Mischenko, M., I. V. Geogdzhayev, L. Liu, A. A. Lacis, B. Cairns, L. D. Travis (2009), Toward unified satellite climatology of aerosol properties: What do fully compatible MODIS and MISR aerosol pixels tell us?, Journal of Quantitative Spectroscopy and Radiative Transfer 110, 402-408, doi:10.1016/j.jqsrt.2009.01.007.
38. Myhre, G., Y. Govaerts, J.M. Haywood, T. K. Bernsten, A. lattanzio (2005), Radiative effect of surface albedo change from biomass burning, Geophysical Research Letters 32, L20812, doi:10.1029/2005GL022897.
39. Nguyen, H. (2009), Spatial statistical data fusion for remote-sensing applications, Thesis, University of California Los Angeles, available at http://theses.stat.ucla.edu/104/Data_fusion_Hai_Nguyen.pdf
40. Paradise, S., B. Wilson and A. Braverman (2009), The Aerosol Measurement and Processing System (AMAPS), Earth Science Informatics, doi:10.1007/s12145-009-0042-7.
41. Penner, J. E., et al. (2002), A comparison of model- and satellite-derived optical depth and reflectivity, Journal of Atmospheric Sciences 59(3), 441±460.
42. Prasad, A. K. and R. P. Singh (2007), Comparison of MISR-MODIS aerosol optical depth over the Indo-Gangetic basin during the winter and summer seasons (2000-2005), Remote Sensing of Environment 107(1-2), doi:10.1016/j.rse.2006.09.026, 109±119.
43. Remer, L. A., D. Tanré, Y. Kaufman, R. Levy, and S.Mattoo, Algorithm forRemote Sensing of Tropospheric Aerosol From MODIS: Collection 005, (2009) Rev. 2, 97 pp. [Online]. Available: http://modis-atmos.gsfc.nasa.gov
44. Remer, L. A., R.G. Kleidman, R.C. Levy, Y.J. Kaufman, D. Tanre, S. Mattoo, J.V. Martins, C. Ichoku, I. Koren, H. Yu, and B.N. Holben (2008), Global aerosol climatology from the MODIS satellite sensors, J. Geophys. Res. 113, doi:10.1029/2007JD009661.
45. Remer, L. A., Y.J. Kaufman, D. Tanre, S. Mattoo, D.A. Chu, J.V. Martins, R.-R. Li, C. Ichoku, R.C. Levy, R.G. Kleidman, T.F. Eck, E. Vermote, and B.N. Holben (2005), The MODIS aerosol algorithm, products, and validation, Journal of Atmospheric Sciences 62, 947±973.
46. Vermote, E. F., J. C. Roger, A. Sinyuk, N. Saleous, and O. Dubovik (2007), Fusion of MODIS-MISR aerosol inversion for estimation of aerosol absorption, Remote Sensing of Environment 107(1-2), doi:10.1016/j.rse.2006.09.025, 81±89.

47. Xiao, N., T. Shi, C. A. Calder, D. K. Munroe, C. Berrett, S. R. Wolfinbarger, D. Li, (2009), Spatial characteristics of the difference between MISR and MODIS aerosol optical depth retrievals over mainland Southeast Asia, Remote Sensing of Environment 113, doi:10.1016/j.rse.2008.07.011,1-9.
48. Yu, H., et al. (2006), A review of measurement-based assessments of the aerosol direct radiative effect and forcing, Atm. Chem. Phys. 6(3), 613-666.
49. Zapletal, M. (2001), Atmospheric deposition of nitrogen and sulphur compounds in the Czech Republic, Scientific World Journal 1(2), 294-303.

TABLES

Table 1- Test case specifications

Test Case	Time Period	Spatial Extent	Estimation Resolution		Number of AERONET locations
			Spatial	*Temporal*	
Eastern	Fall	70°-85°W 25°-50°N	0.2° x 0.2°	Average over a 7 day period	10
Western	Summer	105°-120° W 25°-50° N	0.2° x 0.2°	Average over a 7 day period	8

Table 2 ± Correlation coefficients between AERONET measurements and MISR and MODIS observations classified by region (Figure 1), and season for the year 2001. Low correlation coefficient (0-0.5) cases are shaded in dark gray, medium correlation coefficient (0.5-0.75) cases are shaded in light gray, and high correlation coefficient cases (0.75-1.00) are in bold. The lowest correlations occur in the west, where bright surfaces and mixtures of spherical particles and non-spherical dust dominate, and in the winter months, when total-column AOT tends to be low, and AOT is near the sensitivity limit of the satellite instruments.

	Winter (DJF)		**Spring (MAM)**		**Summer (JJA)**		**Fall (SON)**		**All Months**	
	MISR	MODIS	MISR	MODIS	MISR	MODIS	MISR	MODIS	MISR	MODIS
Western	0.49	0.09	0.67	0.29	0.47	0.32	0.59	0.09	0.63	0.30
Central	**0.92**	0.51	0.68	0.61	0.73	0.58	0.67	0.43	**0.80**	0.59
Eastern	**0.79**	0.70	0.52	**0.77**	**0.86**	**0.87**	**0.82**	**0.80**	**0.78**	**0.84**

Table 3 - Drift coefficient values, their associated uncertainties and the coefficient of variation for the two test cases from the universal kriging model.

Test Case	Constant			**MISR**			**MODIS**		
	$\ddot{O}_0$	$\sigma_{\ddot{O}_0}$	$\sigma_{\ddot{O}_0} / \ddot{O}_0$	$\ddot{O}_1$	$\sigma_{\ddot{O}_1}$	$\sigma_{\ddot{O}_1} / \ddot{O}_1$	$\ddot{O}_2$	$\sigma_{\ddot{O}_2}$	$\sigma_{\ddot{O}_2} / \ddot{O}_2$
Eastern	0.010	0.014	1.4	0.017	0.16	9.42	0.68	0.12	0.18
Western	0.027	0.024	0.88	0.37	0.16	0.43	0.040	0.070	1.75

FIGURES

Figure Captions

Figure 1 - Location of AERONET sites used in the correlation analysis. The examined regions are outlined in blue. Closed circles represent observation locations also used in the universal kriging test cases.

Figure 2 ± AERONET sites used for Western and Eastern test case. The AERONET sites in the Western Region are Missoula (MIS), Rimrock (RIM), BSRN-BAO-Boulder (BSR), Railroad Valley (RAI), Rogers Dry Lake (ROG), La Jolla (LAJ), Maricopa (MAR) and Sevilleta (SEV); the AERONET sites in the Eastern Region are Rochester (ROC), Cartel (CAR), Harvard Forest (HVF), GISS (GIS), Philadelphia (PHI), MD Science Centre (MDS), GSFC (GSF), Big Meadows (BIG), Wallops (WAP) and Cove (COV).

Figure 3 - Variograms of the spatial and temporal variability of AOT from MISR and MODIS. Panels (a) and (b) represent the spatial and temporal variograms of AOT over a 16 day period from April 11 to April 26, 2001 for MISR and MODIS respectively. The color bar indicates the semi-variance. Panels (c) and (d) represent the spatial variogram over the same period from MISR and MODIS, respectively, using all data over the 16-day period. Panels (e) and (f) show the correlation length (*3l*) and variance of AOT for all 16-day periods in 2001 for MISR and MODIS, respectively. Note that MODIS had no data for one repeat cycle in June.

Figure 4 - Comparison of AOT_{OK} with AOT_{UK} for Eastern Test Case for one period from October 29 to November 4. The black asterisks indicate the locations of the AERONET sites. The white gaps indicate the 7-day satellite coverage mask that is imposed on both universal and ordinary kriging for ease of comparison. (a) Best estimates obtained from ordinary kriging. (b) Uncertainty associated with the ordinary kriging estimates. (c) Best estimates obtained from universal kriging. (d) Uncertainty associated with the universal kriging estimates.

Figure 5 - Comparison of AOT_{OK} with AOT_{UK} for Western Test Case for a 7-day period from July 21 to July 27. The black asterisks indicate the locations of the AERONET sites. The white gaps indicate the 7-day satellite coverage mask that is imposed on both universal and ordinary kriging for ease of comparison. (a) Best estimates obtained from ordinary kriging. (b) Uncertainty associated with the ordinary kriging estimates. (c) Best estimates obtained from universal kriging. (d) Uncertainty associated with the universal kriging estimates.

Figure 6 ± Cross validation results for October 29 ± November 4 for Eastern test case. Error bars UHSUHVHQW□□

SUPPLEMENTARY MATERIAL

Figure Captions

Figure S1 ± Cross-validation results for September 3 to October 14, 2001 for Eastern test case. Error bars UHSUHVHQW□□

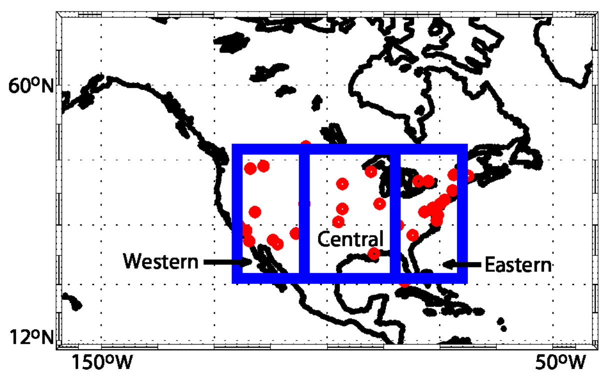

60°N
12°N
150°W
50°W
Western
Central
Eastern

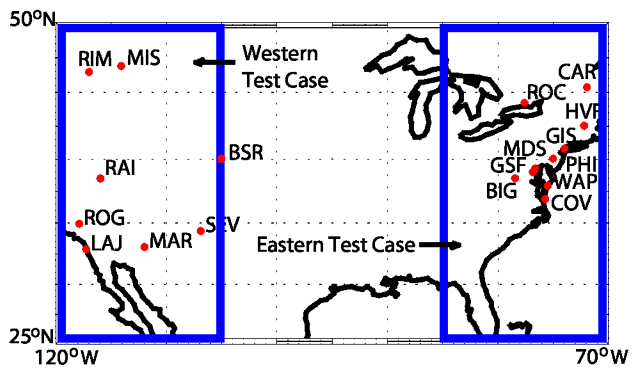

50°N
25°N
120°W
70°W
Western
Test Case
Eastern Test Case
RIM
MIS
BSR
RAI
ROG
LAJ
MAR
SEV
CAR
ROC
HVF
GIS
MDS
GSF
PHI
BIG
WAP
COV

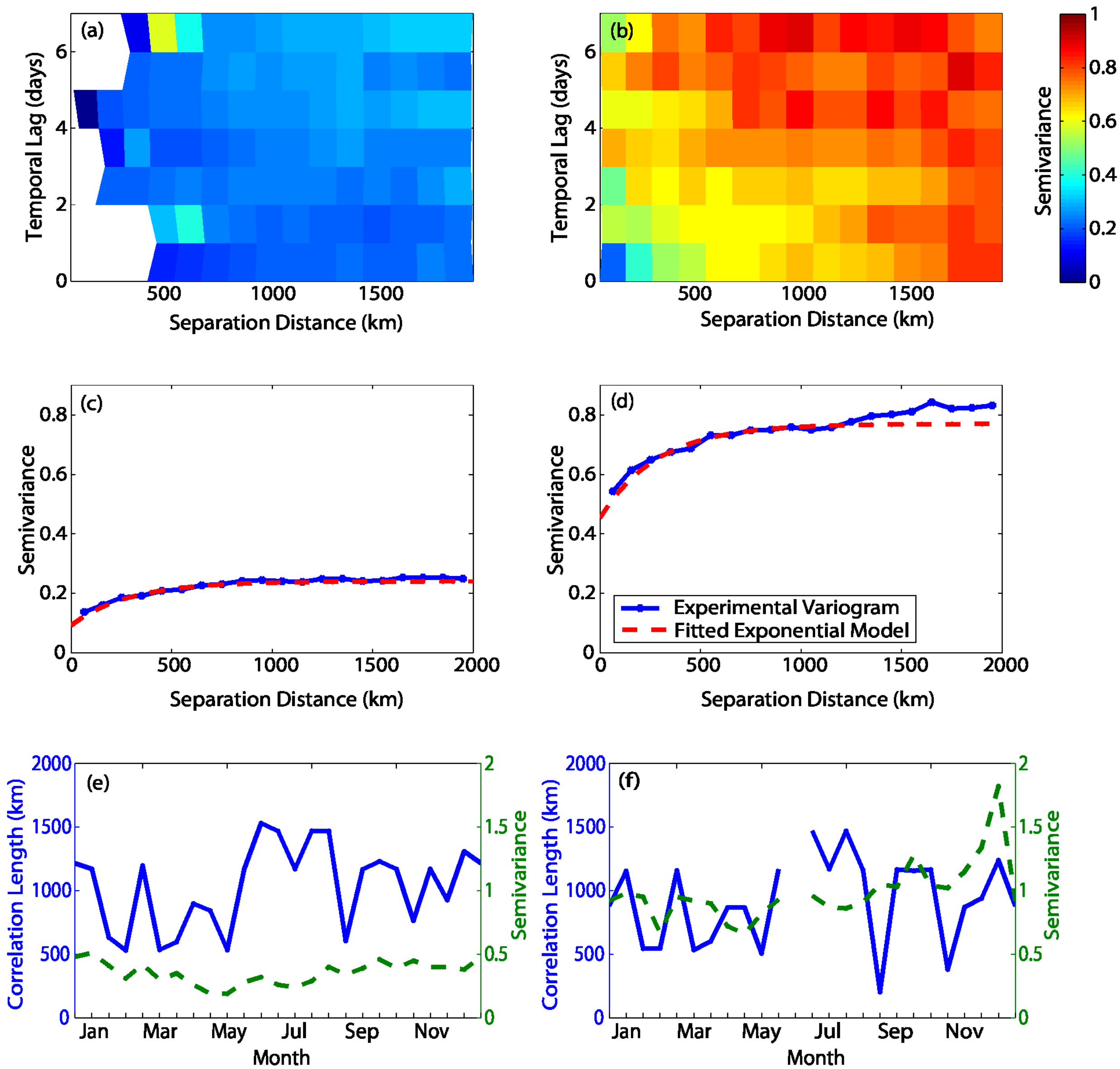

(a)
(b)
(c)
(d)
(e)
(f)
Temporal Lag (days)
Separation Distance (km)
Semivariance
Experimental Variogram
Fitted Exponential Model
Correlation Length (km)
Month
Jan
Mar
May
Jul
Sep
Nov

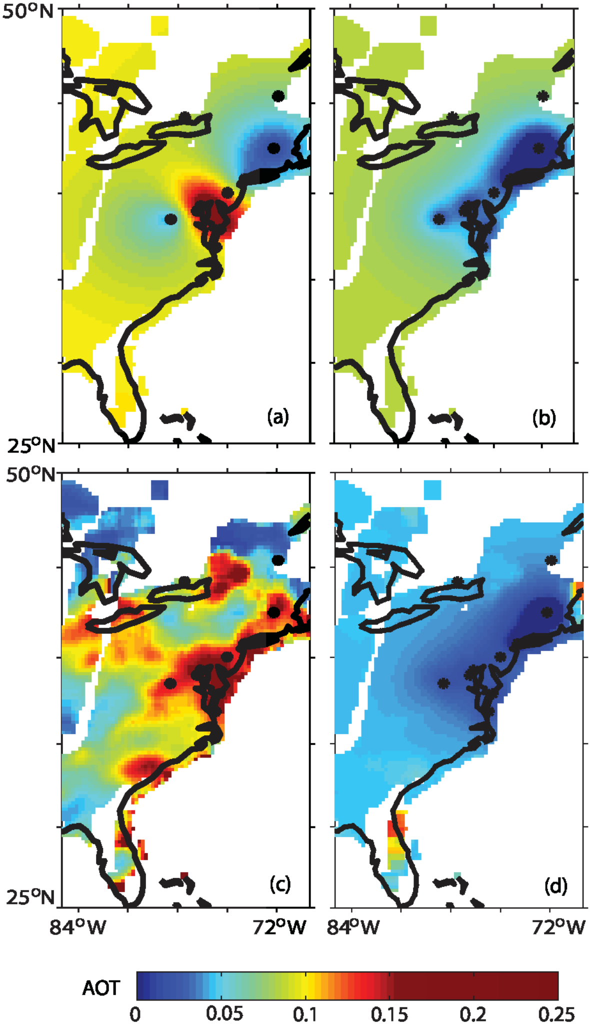
50°N
25°N
50°N
25°N
84°W
72°W
84°W
72°W
(a)
(b)
(c)
(d)
AOT
0
0.05
0.1
0.15
0.2
0.25

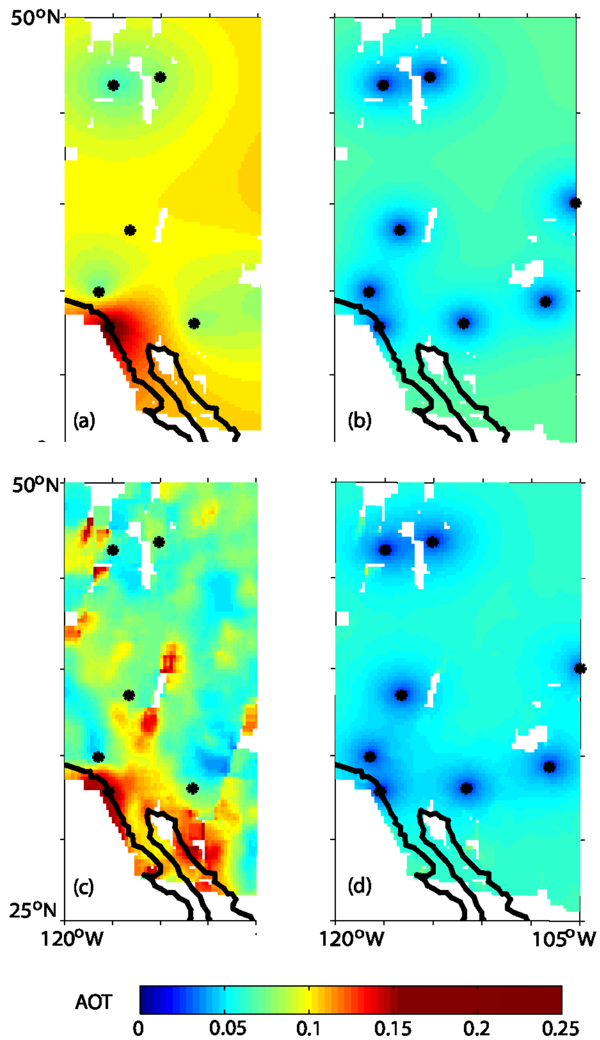

50°N
(a)
(b)
50°N
(c)
(d)
25°N
120°W
120°W
105°W
AOT
0
0.05
0.1
0.15
0.2
0.25

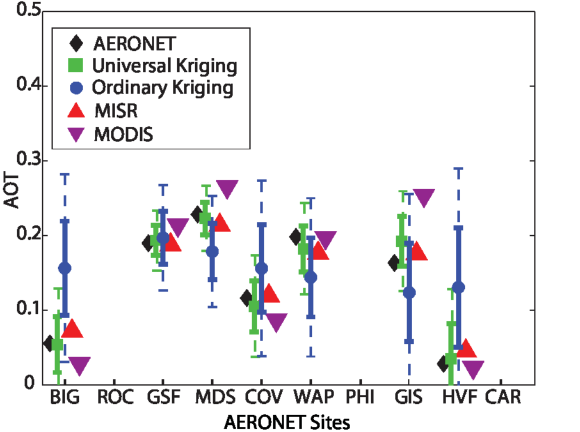

AERONET
Universal Kriging
Ordinary Kriging
MISR
MODIS
AOT
0.5
0.4
0.3
0.2
0.1
0
BIG ROC GSF MDS COV WAP PHI GIS HVF CAR
AERONET Sites

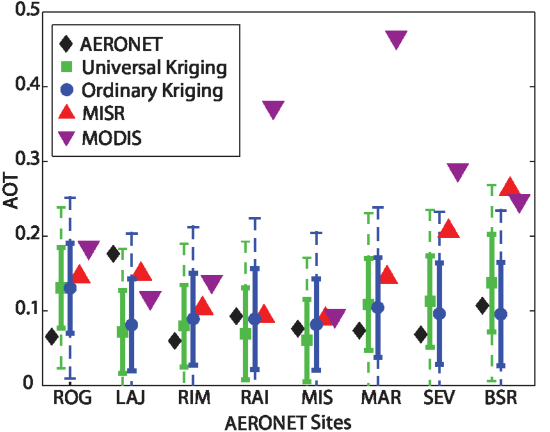
AERONET
Universal Kriging
Ordinary Kriging
MISR
MODIS
AOT
0.5
0.4
0.3
0.2
0.1
0
ROG
LAJ
RIM
RAI
MIS
MAR
SEV
BSR
AERONET Sites